Korean Journal Of Agricultural Science

pISSN : 2466-2402
eISSN : 2466-2410

MANAGEMENT&ECONOMICS

Stress and fatigue analysis of major components under dynamic loads for a four-row tractor-mounted radish collector

Khine Myat Swe[1,†], Md Nasim Reza[1,2,†], Milon Chowdhury[1,2], Mohammod Ali[1], Sumaiya Islam[2], Sang-Hee Lee[3], Sun-Ok Chung[1,2,*], Soon Jung Hong[4,*]

[1]Department of Agricultural Machinery Engineering, Chungnam National University, Daejeon 34134, Korea

[2]Department of Smart Agricultural Systems, Chungnam National University, Daejeon 34134, Korea

[3]National Institute of Agricultural Sciences, Rural Development Administration, Jeonju 54875, Korea

[4]Korea National College of Agriculture and Fisheries, Jeonju 54874, Korea

[†]These authors equally contributed to this study as first author.

[*]Corresponding authors: sochung@cnu.ac.kr, hsj43333@korea.kr

Abstract

The development of radish collectors has the potential to increase radish yields while decreasing the time and dependence on human labor in a variety of field activities. Stress and fatigue analyses are essential to ensure the optimal design and machine life of any agricultural machinery. The objectives of this research were to analyze the stress and fatigue of major components of a tractor-mounted radish collector under dynamic load conditions in an effort to increase the design dependability and dimensions of the materials. An experiment was conducted to measure the shaft torque of stem-cutting and transferring conveyor motors using rotary torque sensors at different tractor ground speeds with and without a load. The Smith-Watson-Topper mean stress equation and the rain-flow counting technique were utilized to determine the required shear stress with the distribution of the fatigue life cycle. The severity of the operation was assessed using Miner's theory. All running conditions produced more than 10^7 of high cycle fatigue strength. Furthermore, the highest severity levels for motor shafts used for stem cutting and transferring and for transportation joints and cutting blades were 2.20, 4.24, 2.07, and 1.07, and 1.97, 3.81, 1.73, and 1.07, respectively, with and without a load condition, except for 5.24 for a winch motor shaft under a load. The stress and fatigue analysis presented in this study can aid in the selection of the most appropriate design parameters and material sizes for the successful construction of a tractor-mounted radish collector, which is currently under development.

Key words: agricultural machinery, fatigue analysis, field load, mechanical life, radish harvester

Citation: Swe KM, Reza MN, Chowdhury M, Ali M, Islam S, Lee SH, Chung SO, Hong SJ. Stress and fatigue analysis of major components under dynamic loads for a four-row tractor-mounted radish collector. Korean Journal of Agricultural Science 49:269-284. https://doi.org/10.7744/kjoas.20220024

Received: February 28, 2022

Revised: April 22, 2022

Accepted: April 26, 2022

Introduction

Radishes (*Raphanus raphanistrum* subsp. *sativus*) are a vegetable widely grown throughout the world, particularly in South Asian countries like Korea, Japan, and China. The annual radish production in Korea was 0.365 and 0.467 million tons in 2020 and 2021, respectively, which was a 9.8% increase in total production (KOSTAT, 2021). Radishes are cultivated in open fields as an annual or biannual crop, and are a good source of vitamins, minerals, and other nutrients (Chowdhury et al., 2021). In many countries, radish cultivation is declining due to labor-intensive and time-consuming cultivation, aged labor with high labor expenses, and limited automation. Field operations such as cultivation and harvesting demand a significant number of human resources. The most labor-intensive activities involve manually picking, gathering, and packing radishes (Jang et al., 2021; Reza et al., 2021; Swe et al., 2021a). Due to significant economic and industrial expansion in the Republic of Korea, agricultural mechanization has been implemented in an effort to alleviate the scarcity of agricultural employees. The mechanization rate of all major upland crops reaches an average of 50%, but the rate of sowing, transplantation, and harvest stages (i.e., where labor is most concentrated) is only 6.7, 7.2, and 25.8%, respectively, and in the case of the harvesting stage, the mechanization rate may decrease by up to 8.9%, which is the lowest rate among all upland crops (Yoo and Hwang, 2018). Therefore, radish collectors are in desperate need of mechanization through the use of agricultural machinery to reduce time and reliance on human labor throughout various field operations.

Continuous attempts to improve agricultural machinery have inspired numerous studies, and it is necessary to pay close attention to all of the factors involved in this issue. Research has been carried out in order to produce a range of harvesters for upland crops, with the goal of reducing crop management problems while simultaneously maximizing crop yield. Yaegashi et al. (2001) designed a radish harvester after analyzing its performance in various field conditions, and Guolong et al. (2016) developed a radish harvester based on a digging shovel model developed by theoretical analysis to achieve the finished harvester. Different types of radish harvesters are being studied for future improvement; researchers want to learn more about the ideal configurations for the conveyor and depth controlling plate, as well as the digging conveyor, primary and secondary cutting blade, and gearbox through the use of field tests (Jung et al., 2018). Particularly, research on the self-propelled radish harvester was not conducted in Korea, but was developed as a tractor-attached type. In light of how many radishes are grown in Korea and how the land is used, it is important to continue developing the self-propelled radish harvester (Kook et al., 2021).

Fatigue life is described as how long an object or substance will last before it completely breaks down due to stress, and is usually calculated as the amount of stress cycles that an entity or material may endure before the damage is done. Fatigue life relies on the running characteristics, model parameters, substance features, and load conditions (Köksal et al., 2013; Swe et al., 2021b). Researchers were introduced to the load spectrum from which the failure life of a machine substance could be estimated. For the purpose of counting the cycles of the observed load loops, the rain flow cycle-counting technique was considered with the sequence effect (Jung et al., 2000).

Due to repetitive loading, components of a tractor-mounted radish collector will propagate a fatigue crack in a high-stress zone until ultimate breakage occurs (Milan et al., 2020; Islam et al., 2021). Upland farm machines such as the onion harvester (Shin et al., 2019) have been improved and utilized in trials based on normal working speed during operation. Strain was measured from 8 different points of a tractor-linked onion harvester and converted into stress in order to achieve the optimum safety factor. Gujar and Bhaskar (2013) presented the fatigue life prediction based on finite element analysis (FEA). The motor shaft is a rotating device, and the stress on a particular spot of the motor shaft changes as the shaft rotates, creating fatigue in the shaft.

Agricultural machinery, especially tractors and various tractor-mounted components, frequently uses welding joints. The material is heated and then cooled throughout the welding process. Physical and chemical differences result in the formation of holes and hollows due to the fundamental components being melted and merged with the filled product. The cross section of the welded joints without a base produce a large range of stress, which leads to fatigue damage of the joint (Eggert et al., 2012).

The tangential tensile stress zone on circular cutting blades used in agricultural machines can increase the circular blade's longevity (Li et al., 2015). To ensure dependability, the narrow, circular saw blade requires a higher tangential tensile stress and a lower radial compressive tensile stress. The implications of strain on the blades' dynamic dependability warrant investigation (Zhang et al., 2014; Gospodaric et al., 2015). The radish collectors' operational parameters were focused on annual working hours, working velocity, stress, load distribution, and fatigue life.

A tractor-mounted radish collector is under development, and the major components of the collector require evaluation in terms of mechanical properties and fatigue life in order to effectively run the collector throughout a suitable service life-range. The analysis of the major functioning components of the harvesters considered as a whole is still in its early stages and requires more research. Therefore, the objectives of this study are to analyze the stress and fatigue of motor shafts for the stem-cutting conveyor belt, transfer conveyor belt, winch motor shaft, transportation joint, and circular cutting blade of radish collectors, and to forecast the expected service life, design, and dimension of the materials.

Materials and Methods

Structure and working procedure of the radish collector under development

Fig. 1 shows the 3D model of the radish collector which was attached to the tractor during the field test, and Fig. 2 illustrates the tension forces on the transfer conveyor of the collector. The collector is composed of 8 key components: the stem-cutting conveyor, transfer conveyor, three hydraulic motors for conveyor belts and stem-cutting, direct current (DC) winch motor, and two furrow guides. Traditionally, farmers harvested radishes by placing them on the stem-cutting conveyor. The radishes were then carried through the transfer conveyor, where polypropylene bags were positioned at the end to collect them, after which the full bags were moved to the desired location. The winch motor was used to fold and unfold the stem-cutting conveyor before and after the operation. The mass of the prototype collector was 460 kg, and the dimensions were 4.21 m × 1.20 m × 2 m (L × W × H), respectively. The average mass and length of the radishes were between the range of 0.14 to 2.27 kg and 0.15 to 0.61 m, respectively.

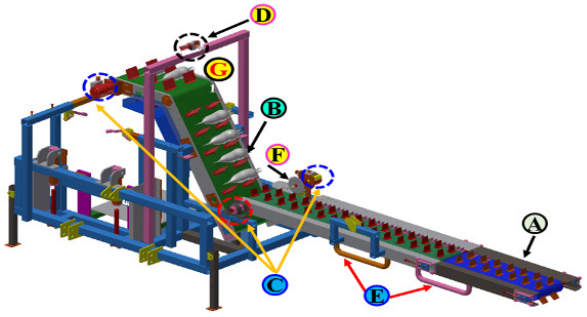

Fig. 1. 3D model of the radish collector under development (A) stem-cutting conveyor, (B) transfer conveyor, (C) hydraulic motors, (D) DC winch motor, (E) furrow guides, (F) stem-cutting blade, and (G) transportation joint.

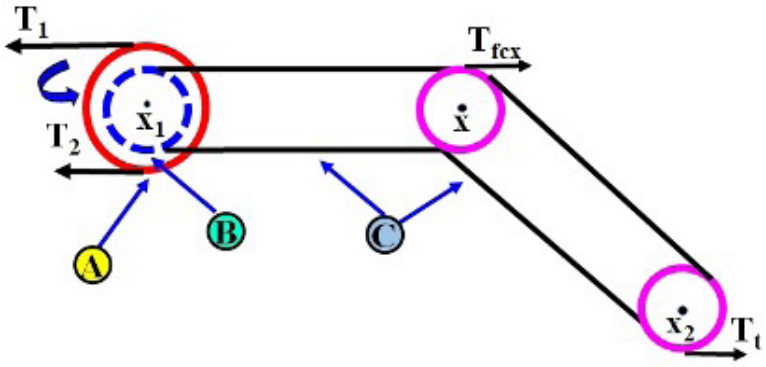

Fig. 2. Schematic diagram of tension forces on the transfer conveyor (A) hydraulic motor, (B) drive pulley, and (C) conveyor belt. x, x_1, and x_2 are the center of the drive pulley. T_1, T_2, T_t, and T_{fex} are the tension forces acting on the driver pulley.

Procedures for stress behavior and severity level of the components

An experimental study was conducted to determine the shaft torque of belt motors used in the stem-cutting and transferring conveyors. Considering field condition, the stress behavior of two motor shafts for two conveyors and a winch, transportation joint, and stem-cutting blade were determined with and without load conditions. For the appropriate shear stress with distribution of fatigue life cycles, the Smith-Watson-Topper mean stress equation and the Rain-flow-counting method were evaluated. Miner's rule was used to determine the severity of the operation by calculating the ratio of the total damage fraction.

Experimental torque measurement of hydraulic motor shafts

Power is transmitted by a shaft, which is a rotating part with a circular cross-section. Rotor system failures are frequently caused by a fatigue fracture in a hydraulic motor's rotating shaft. For long-term functioning of the machine components, the significant results will guide the protection model and anticipate the fatigue lifecycles (Niu and Yang, 2018).

This study was supervised by the Department of Agricultural Machinery Engineering in the College of Agriculture and Life Sciences at Chungnam National University, and the Daejeon and Rural Development Administration (RDA) in South Korea. The experiment was carried out on August 7th, 2019, and the experimental site was located at Pyeongchang-gun, Gangwon-do, South Korea. The experiment was performed on a test area of 800 m^2, where radishes (*Raphanus sativus*) were grown. At the time of harvest, the field appeared to be in good condition.

Two torque sensors (Futek TRS-605, California, USA) were connected to two 12 kW motors (MP250, Kazanluk, Bulgaria) via the LabVIEW (National Instruments Corp., Austin, Texas, USA) data acquisition (DAQ) system, which included programs for rotational speeds of 42, 87, and 112 rpm, as well as for loaded and unloaded conditions. The experiment was carried out using tractor forward speeds of 1.36, 1.55, and 1.73 $km \cdot h^{-1}$ and an engine power of 52 kW. Each trial was carried out three times under identical conditions.

Analysis of stress behavior of conveyor motor shafts

American Society for Testing and Materials (ASTM) standard for SCM420H carbon steel was used to replicate the S-N correction data of the motor shafts for various operating and tractor ground speeds in both loaded and unloaded conditions by equation (1) (Kim et al., 2013).

$$N = 10^{\left(6-6.097\log\left(\frac{S}{223}\right)\right)} \quad (1)$$

Where, N is the number of cycles and S is the shear stress (MPa).

The tensile and fatigue strengths of the substance were assumed to be 1,817 MPa and 700 MPa, respectively (Lee et al., 2018). The effects of the radish collector operations on the fatigue life of the motor shafts were evaluated using the partial damage theory, and were compared in terms of severity level on the material's fatigue strength. The equivalent torque of the load spectrum was transformed into shear stress using equation (2) (Petracconi et al., 2010).

$$S = \frac{16T_e}{\pi D^3} \quad (2)$$

Where, S is shear stress (MPa), T_e is the equivalent torque (Nm), and D is the shaft diameter (mm).

Stress approach of winch motor shaft

The stem-cutting conveyor was folded vertically onto the winch frame in its typical configuration. A 0.12 kW DC winch motor (H9D12-120D, Korea Hoist Co., Ltd., Ansan, Korea) was used to drive the stem-cutting conveyor into a horizontal position while the tractor-mounted radish collector was in use. The winch motor's shaft torque was calculated using equation (3) (Matejic et al., 2013). The equivalent torque under the folded or unfolded stem-cutting conveyor was used to calculate the shear stress and lifespan of the winch motor shaft, which was the same method used for the conveyor motors' shafts.

$$M_w = \frac{P_w \times \eta_B^2}{\omega_w} \quad (3)$$

Where, M_w is the torque of the winch motor shaft (Nm), P_w is the calculated hydraulic power of the winch motor (0.3, 0.7, 1.1 and 1.4 kW), $_w$ is the radial velocity of the winch motor (0.9, 1.4, 2, and 2.2 rad·s^{-1}), η_B is the efficiency ratio of the drum bearings (1), and D_w is the shaft diameter of the winch motor (16 mm).

Analysis of stress behavior of transportation joint

Welding was used to attach the transportation joint of the transfer conveyor (Fig. 1), as dynamic components of equipment can result in serious injuries and fatalities when subjected to repetitive load and oscillation. Tensile strength was tested on the transportation conveyor belt. Torsional stiffness is greatly increased in beams with non-circular cross sections when the end portions are wrapped with stiff blocks (Wikipedia, 2021). The deflection and torsion constant of joint elements were calculated from the measured torque results using equations (4) and (5) under loaded and unloaded conditions.

$$\delta = \frac{F_j \times a_j}{A_j \times E_j} \quad (4)$$

$$J = \beta a_J b_J^3 \quad (5)$$

Where, δ is the deflection (mm), F_j is the applied force (294.3 N), a_j is the long length of the joint component (m), A_j is the area of the joint component (m^2), E_j is the elastic modulus of the joint (MPa), J is the torsional constant, b_j is the short length of the joint *component* (m), β is the numerical factor depending on the ratio of a_j/b_j (0.299), T_e is the equivalent torque (Nm), and S_j is the maximum shear stress of the joint (MPa).

The Basquin equation was utilized in accordance with the ASTM standard for S275 mild steel to assess stress versus cycle-to-failure data for the transportation joint material (Piotr, 2011). Yield strength and modulus of elasticity were 0.275 and 40 GPa, respectively, for the S275 mild steel. To determine the damage, we used equations (6) and (7) to adjust the material's shear stress from the corresponding torque with load spectrum.

$$S_j = \frac{T_e \times a_j}{J} \tag{6}$$

$$N = 10^{-14.49 \log S + 37.93} \tag{7}$$

Where, S_j is the maximum shear stress of the joint (MPa), T_e is the equivalent torque (Nm), J is the torsional constant, a_j is the long length of the joint *component* (m), Nis the number of cycles, and S is shear stress (MPa).

Analysis of stress nature of stem-cutting blade

At the end of the stem-cutting conveyor, a blade for cutting radish stems was attached. When the radish was put onto the conveyor, the stem was clipped using a circular spinning blade operated by a hydraulic motor. Tangential compressive stress and deformation are created at the edge of the circular blade as a result of the central force created by the blade's operating speed. When the stem cutting force is delivered to the cutting blade, the circular blade's tangential stress and deformation can be calculated using equations (8 - 12) through the linear fitting approach (Li et al., 2015).

$$m = 0.112(P_b - 35) + 6.96 - 0.016(r_b - 60) \tag{8}$$

$$\sigma_{\theta t} = k_0(m, r_b) \tag{9}$$

$$k_0(m, r_b) = f_0(r_b)(m - 6) + C_0(r_b) \tag{10}$$

$$f_0(r_b) = 9.160 \times 10^{-5} r_b^3 - 0.026 r_b^2 + 2.399 r_b - 72.459 \tag{11}$$

$$C_0(r_b) = 1.870 \times 10^{-4} r_b^3 - 0.052 r_b^2 + 4.862 r_b - 146.449 \tag{12}$$

Where, $\sigma_{\theta t}$ is the radial compressive stress (MPa), k_0 is the coefficient of function (m, r_b), P_b is the blade-driving force (8, 16, 24, 32, 40, and 48 N), m is the deformation (mm), r_b is the radius of the stem-cutting blade (0.08 m), and f_0 and C_0 are the coefficients of function (r_b).

The relationship between stress and strain was expressed by equation (13) using power law hardening proposed by Hollomon (Hollomon, 1945). The process of fatigue life with amplitude of elastic strain was described using equation (14) on Ti alloy IMI 834 material (Singh and Singh, 2002).

$$\sigma_{\theta t} = K \varepsilon_p^n \tag{13}$$

$$N_b = \frac{1}{2} \times 10^{\log \frac{E \Delta \varepsilon_p}{2 \sigma_f}} \tag{14}$$

Where, K is the strength coefficient of the material (1310.5), ε_p is the amplitude of elastic strain, n is the hardening exponent of strain (0.0463), N_b is fatigue life cycles of the cutting blade, E_b is the blade modulus of elasticity (200 GPa), b_b is the burgers vector (0.036), and σ_f is the fatigue strength coefficient (1,200).

Severity calculation of damage for the collector

The conveyor's workload was investigated using the motor shaft's load signal as torque, stress amplitude, and damage ratios associated with the load spectrum of loaded and unloaded conditions. By subtracting the influence of mean torque, the Smith-Watson-Topper mean stress equation and Rain-flow cycle counting technique were used to determine the appropriate shear stress with distribution of fatigue life cycles and magnitude of load spectrum (Aldeeb and Abduelmula, 2018). Torque magnitude and the total number of fatigue life cycles of the collector's whole life were computed using equations (15) and (16).

$$T_e = \sqrt{(t_m + t_a)\, t_a} \tag{15}$$

$$N_T = 3{,}600\ NLh \tag{16}$$

Where, T_e is the effective torque (Nm), t_m is the average torque (Nm), t_a is torque amplitude of measurement (Nm), N_T is the total number of fatigue cycles, N is the number of computed cycles for the load measurement (cycle·s^{-1}), L is the whole life of the collector (year), and h is the annual utilization hour (h·year^{-1}).

The collector's whole life was considered ten years and its working hours was considered 3,000 hours. The severity level of the process was expressed using equation (17) across the ratio of the sum of damage fractions (Bannanttne et al., 1990). The damage sum was determined using measured load and S-N (bending stress vs. the number of cycles) curve to predict the number of cycles of loading to failure (Fatemi and Yang, 1998). The S-N curve was transformed to a torque-cycle curve due to the damage caused by the torque signal (Nguyen et al., 2011). Miner's theory (Miner, 1945) of normalized fatigue referenced the least amplitude of the damage sum at all working velocities.

$$D_t = \sum_{i=1}^{k} \frac{n_i}{N_i} \tag{17}$$

Where, D_t is the damaged sum of the operation, n_i is the number of actually generated cycles at the i^{th} operation condition, and N_i is the theoretical fatigue life cycles at the i^{th} operation condition.

Selected design variables of the collector

For the manufacturer, an efficient design process and effective material handling are essential to create more efficient and cost-effective machinery that may increase agricultural productivity. The design parameters of the collector's model, such as shaft diameters of the stem-cutting conveyor motor (D_s), transferring conveyor (D_t), long length (a_j), and short length (b_j) of the transportation joint, radial speed of the winch conveyor ($_w$), and radius of the stem-cutting blade (r_b) were mentioned in Table 1. Various results for shear stress, fatigue life, and deflection of the components was focused under the loaded condition.

Table 1. Design variables of a 4-row tractor-mounted radish collector.

Item	Unit	Fixed value	Range	Interval value
D_s	m	0.02	0.01 - 0.03	0.02
D_t	m	0.02	0.01 - 0.03	0.02
a_j	m	0.60	0.20 - 1.00	0.20
b_j	m	0.10	0.10 - 0.50	0.10
ω_w	rad·s^{-1}	1.62	0.50 - 2.50	0.50
r_b	m	0.08	0.07 - 0.13	0.005

Results and Discussion

Stress behavior of conveyor motor shafts

The lowest and highest torque magnitude of the motor shafts for stem-cutting and transferring conveyors under the rotational speed of 114 rpm with a tractor forward speed of 1.73 km·h^{-1} were 15.4907 to 19.0922 Nm, 18.2304 to 21.2136 Nm, 13.5853 to 15.9828 Nm, and 16.9853 to 19.9827 Nm, respectively, with and without load conditions. Figs 3 and 4 show the shear stress of motor shafts for stem-cutting and transferring conveyors with and without load conditions. With the same rotational and tractor ground speeds, the smallest and largest shear stress of motor shafts were observed as 3.5231 to 3.7238 $\times$ 10^{-3} MPa, 3.8963 to 4.0350 $\times$ 10^{-3} MPa, 2.7713 to 3.0206 $\times$ 10^{-3} MPa, and 3.3525 to 3.5419 $\times$ 10^{-3} MPa, respectively, with and without load conditions.

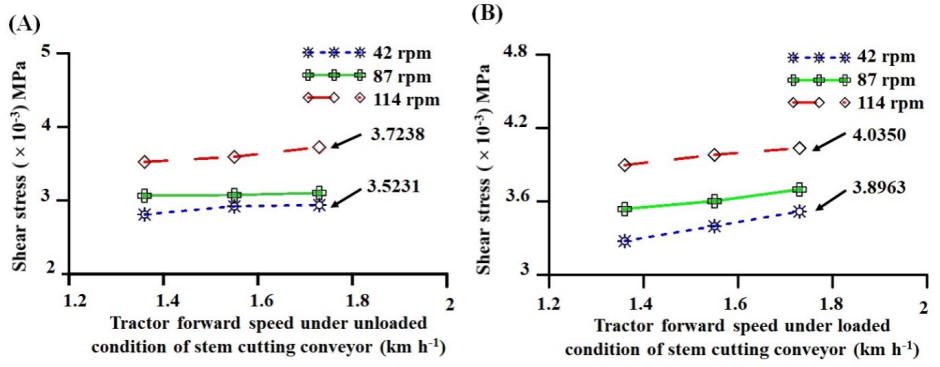

Fig. 3. Shear stress of motor shaft for stem-cutting conveyor with (A) unloaded condition and (B) loaded condition.

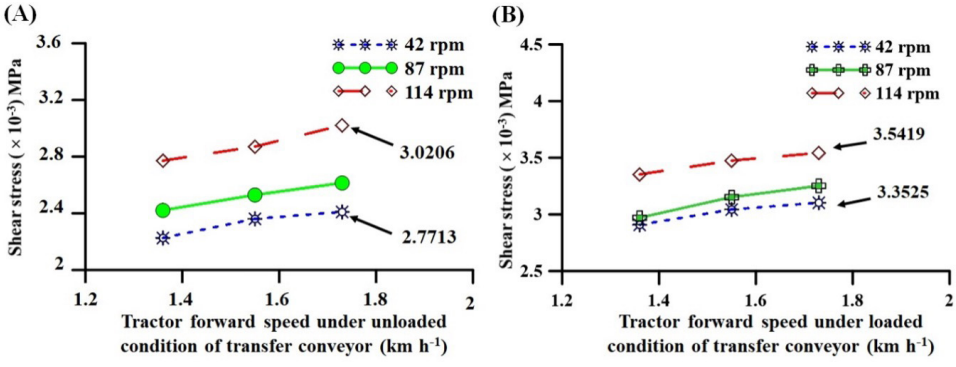

Fig. 4. Shear stress of motor shaft for transfer conveyor with (A) unloaded condition and (B) loaded condition.

The temporal distribution of the stress spectrum and the load history of the motor shafts of stem-cutting and transferring conveyors are shown in Figs 5 and 6 for all operating and tractor speeds with and without load conditions. The motor shafts were capable of establishing over 10^7 cycles under all operating circumstances. For each type of equipment, a fatigue limit of maximum load in ten million cycles is permissible (Miner, 1945).

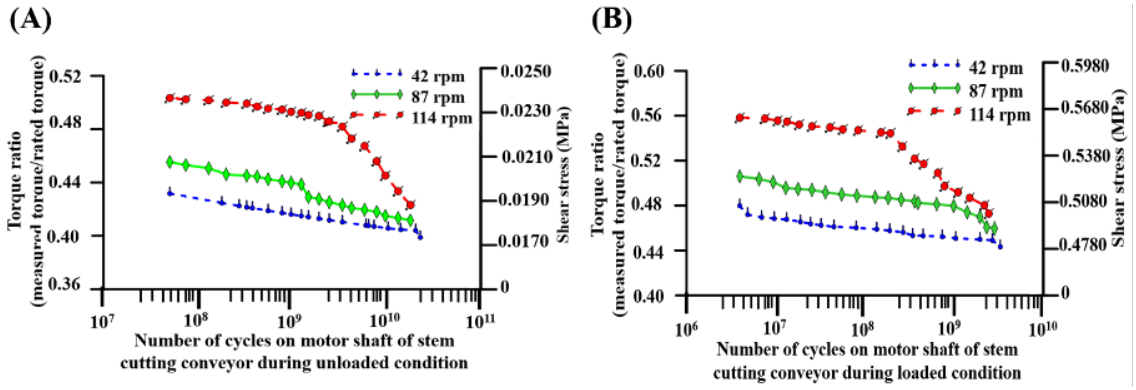

Fig. 5. Load spectrum and S-N curve of motor shaft for the stem-cutting conveyor with (A) unloaded condition and (B) loaded condition.

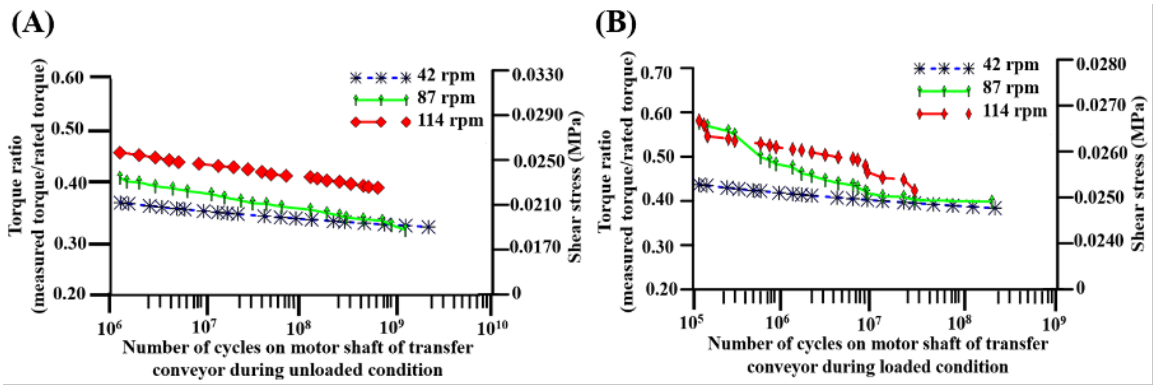

Fig. 6. Load spectrum and S-N curve of motor shaft for the transfer conveyor with (A) unloaded condition and (B) loaded condition.

With and without load conditions, the high cycles to low speed and low cycles to high speed were observed. The largest stress distributions of motor shafts at 114 rpm were 0.0235 to 0.0261 MPa and 0.0206 to 0.0242 MPa, respectively. A stepped cylindrical geometry, loading, stress, and deflection, or material strength and stiffness, are taken into consideration while designing a shaft (Kolgiri et al., 2013). The maximum torque ratios of the motor shafts under the rotational speeds of 42 and 114 rpm were obtained as 0.4318 to 0.5017, 0.4797 to 0.5583, 0.4318 to 0.5017, and 0.4367 to 0.5583, respectively, with and without load conditions.

The corresponding severity of the rotational speeds of two motor shafts is displayed in Fig. 7. The severity levels of shafts for stem-cutting and transfer conveyor belts were 1, 1.97, and 2.20; 1, 1.18, and 1.97; 1, 2.63, and 4.24, and 1, 1.60, and 3.81, respectively, with and without load conditions. When the operational speed was increased, the severity level of the damage sum also increased up to 100 - 424% under different speed and load conditions.

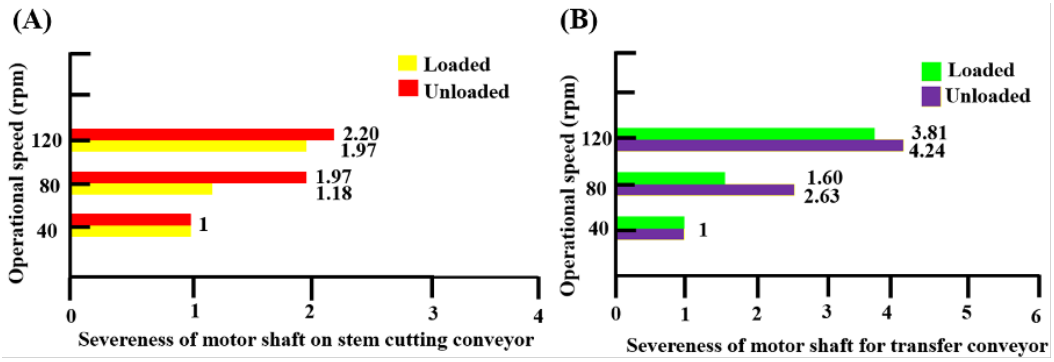

Fig. 7. Damage severity of the motor shaft on (A) stem-cutting conveyor and (B) transfer conveyor.

Stress behavior of winch motor shaft

Fig. 8A shows the relationship between shaft torque and shear stress of the winch motor, and Fig. 8B shows the relationship between shaft torque and damage severity of the winch motor. The lowest and highest shear stress of the winch motor shaft were 0.4192 to 0.8023 MPa at the lowest and highest torque positions under loaded conditions. Damage severity levels of the shaft were attained at 1, 2.47, 5.15, and 5.24 related to the shaft torque of 244, 552, 800, and 1,052 Nm, respectively.

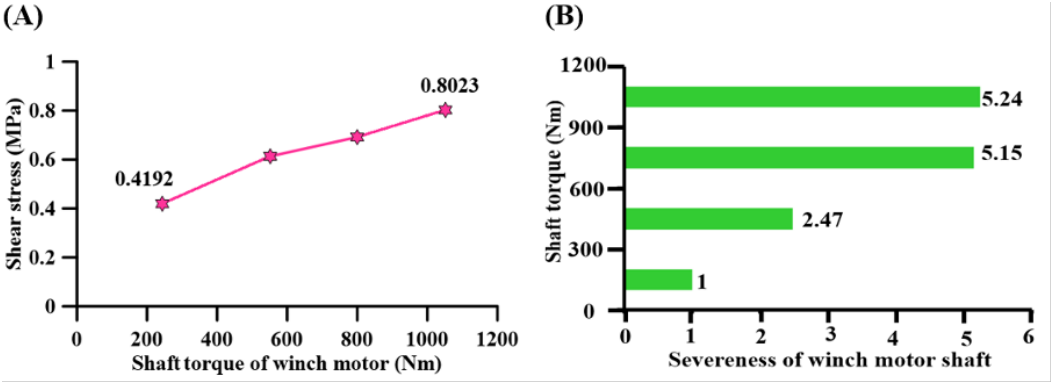

Fig. 8. Relation between shaft torque of winch motor with (A) shear stress and (B) damage severity.

Stress behavior of transportation joint

The shear stress of the transportation joint is shown in Fig. 9. The maximum shear stress was found to be 46 $\times$ 10^{-3} to 77 $\times$ 10^{-3} MPa and 48 $\times$ 10^{-3} to 80 $\times$ 10^{-3} MPa at the rotational speed of 114 rpm and tractor speed of 1.73 km·h^{-1}, with and without load conditions. The impact of uncertain alignments on the fatigue strength of 3 to 4 mm deep butt-welded joints was conducted by using mini-scale samples (Fricke et al., 2015) and panels (Lillemäe et al., 2013). For thin-walled building parts, the welding twist can cause considerable high-to-secondary stresses under external loads (Radaj et al., 2006).

The torque and stress amplitude relationship of a transportation joint was investigated with and without load conditions. The observation revealed that under all working conditions, over 10^7 fatigue life cycles would be generated. The smallest and largest cycles of the joint at 114 and 42 rpm were found to be proportional to the maximum and minimum torque load ratios.

At 114 rpm, the maximum amplitudes of shear stresses were 0.0015 and 0.0844 MPa, respectively. At 42, 87, and 114 rpm, the highest ratios of measured torque to rated torque were around 0.4569, 0.4619, and 0.4805, and 0.4809, 0.4864, and 0.4883.

Various severity levels for the transportation joint were approximately 1, 1.77, and 2.07, and 1, 1.54, and 1.73, respectively, with and without load conditions under the rotational velocities of 42, 87, and 114 rpm. Furthermore, the severity level of the joint corresponds to the rotational velocity, as shown in Fig. 10. When the operating speed was higher, the damage level of the joint was increased by about 100 - 207%, with and without load conditions.

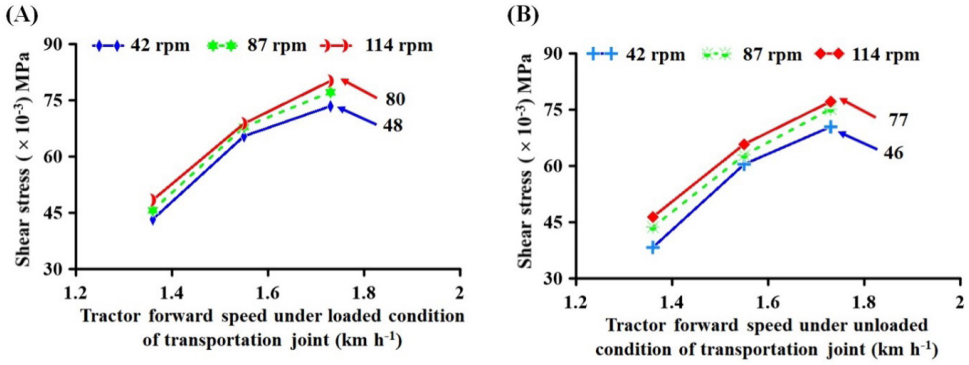

Fig. 9. Shear stress of transportation joint with (A) unloaded condition and (B) loaded condition.

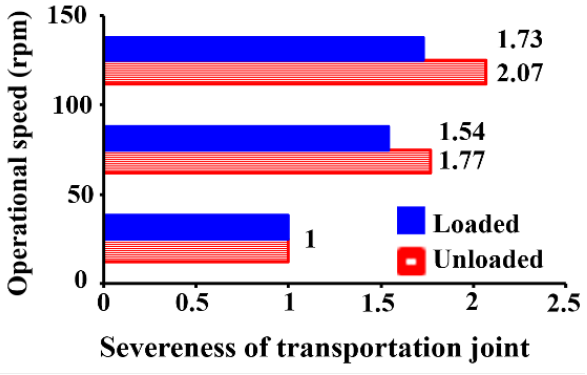

Fig. 10. Variation of severity level for transportation joint with and without load conditions.

Stress behavior of stem-cutting blade

The tangential stress on the stem-cutting blade edge is shown in Fig. 11A. There was a slight increase from 418.6095 to 419.8021 MPa and 418.7884 to 419.8618 MPa by various stem-cutting forces at 8, 16, 24, 32, 40, and 48 N, with and without load conditions. Significant tangential compressive stress at the blade's end results in bucking deflection, which reduces the trimming quality, increases slit waste, and shortens blade life (Li et al., 2015). Fig. 11B shows the damage severity levels of the blade as 1, 1.02, 1.03, 1.05, 1.06, and 1.07, and 1, 1.01, 1.03, 1.04, 1.06, and 1.07, with and without load conditions, respectively.

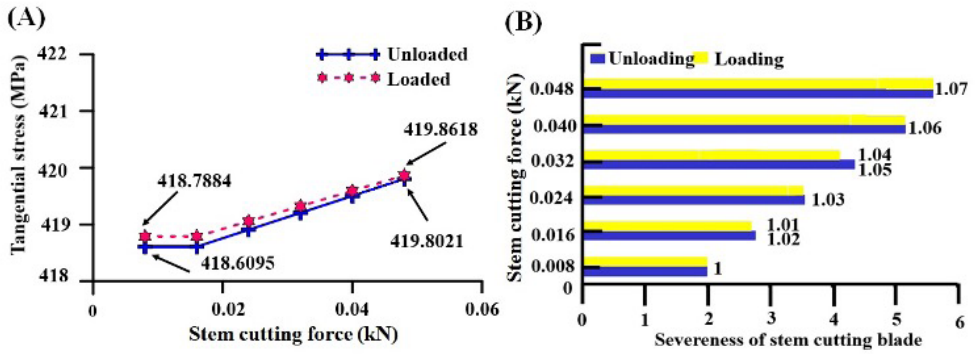

Fig. 11. Relation between stem-cutting force of blade with (A) tangential stress and (B) damage severity, with and without load conditions.

Effects of design variables of the collector

Fig. 12 shows that when the belt motor shaft diameters for stem-cutting and transferring conveyors increased, the shear stress decreased and fatigue life increased. The shear stress decreased continuously between 0.1493 to 0.0055 MPa and 0.1329 to 0.0049 MPa, respectively, and the fatigue life increased up to 3.40×10^{33} and 2.45×10^{33}, respectively. Increasing the winch motor's radial velocity led to an increase of the shear stress on the shaft, however, the number of fatigue cycles decreased, as illustrated in Fig. 13. The shear stress on the winch motor shaft increased from 0.4192 to 0.8024 MPa, while the number of fatigue cycles decreased from 4×10^{24} to 8×10^{19}. Belt width and pulley diameter can be selected based on the accurate diameter of the shaft.

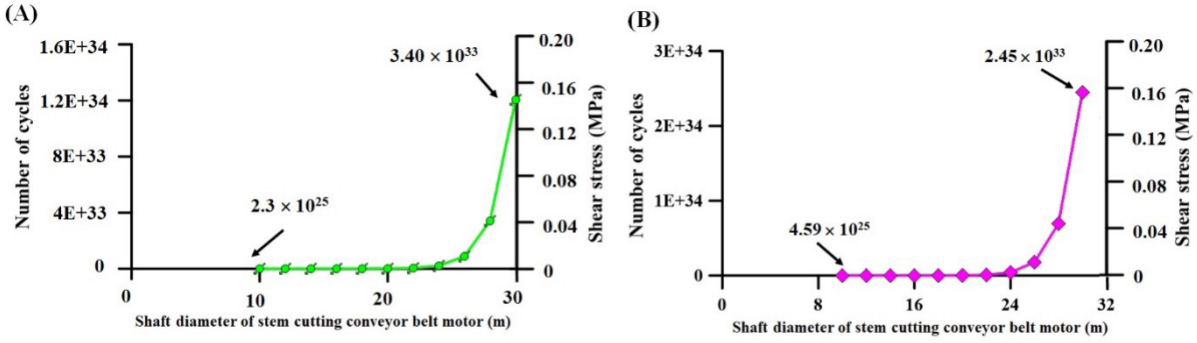

Fig. 12. Relationship between fatigue life cycles and shear stress with (A) stem-cutting conveyor belt motor shaft diameter and (B) transfer conveyor belt motor shaft diameter.

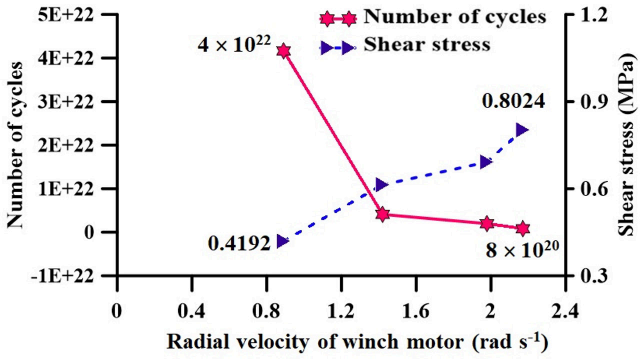

Fig. 13. Variation of fatigue life cycles and shear stress to radial velocity of winch motor shaft.

Considering the design variables of the machine, the optimum design structure can be determined from the fatigue strength of the S-N curve for the transportation joint. The shear stress distribution of the long length side was stable at 0.0840 MPa, but the shear stress distribution of the short length side gradually decreased from 0.0840 to 0.0007 MPa, until it became ignored (Fig. 14A). However, the fatigue life cycles of the transportation joint were fixed at 3.29×10^{53} for both the short and long length sides, but in the case of the short length side, it continuously increased to 8×10^{83} (Fig. 14B). During the stress condition, the deflection of the transportation joint sharply decreased to between 221×10^{-6} to 44×10^{-6} mm and 74×10^{-6} to 15×10^{-6} mm for the long and short length sides, respectively. According to the Korean steel structural design code and commentary (Korean Society of Steel Structure, 2018), a distortion of one-third of the length is considered acceptable. As such, the complete deflection was not obvious.

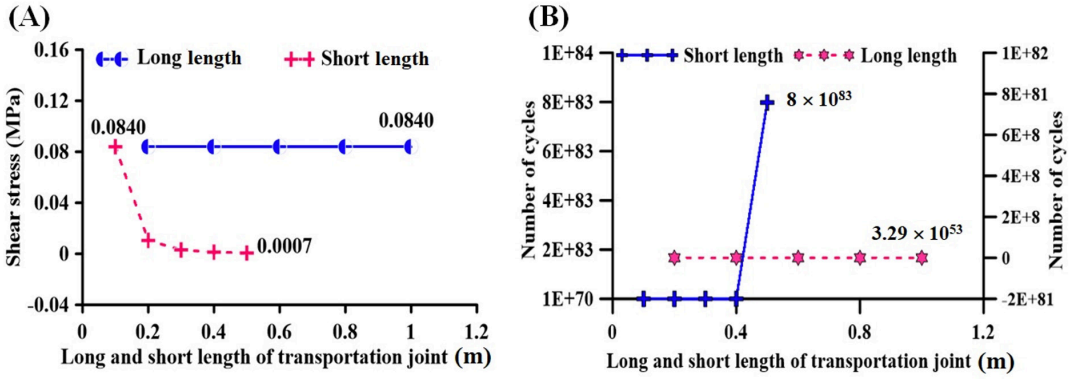

Fig. 14. Variation of long and short length of transportation joint with (A) shear stress and (B) life cycle distribution.

In addition, the tangential stress on the stem-cutting blade was between 223 and 1,608 MPa, but the number of cycles decreased from 4.3×10^{17} to 2.78×10^{6} with the increase of the blade radius as shown in Fig. 15. Deflection of the blade varied from 2.88 to1.92 mm, which was insignificant. The tangential shear stress was surveyed using an X-ray stress meter for three different types of circular saw blades (Umetsu et al., 1994).

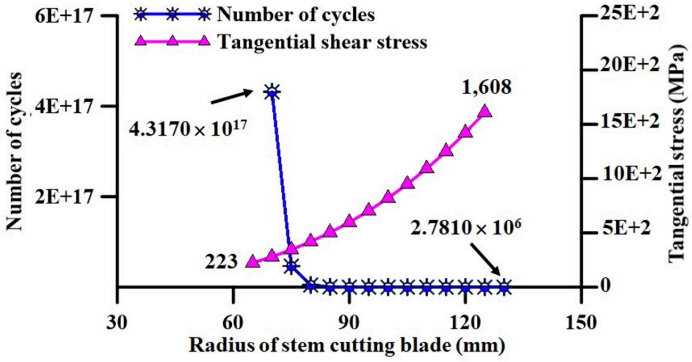

Fig. 15. Variation between tangential shear stress and fatigue life cycles to radius of stem-cutting blade.

The experimental findings demonstrated that even when the tension between the components is negligible, a fatigue study is necessary (1 MPa or less). However, repetitive low-level loading may develop and expand a fatigue fracture at a stress concentration, eventually resulting in failure or even deformation. Fatigue fractures usually begin at stressors, and in the case

of agricultural machinery, even a small amount of fatigue may result in significant damage later on. As a result, eliminating such faults boosts fatigue strength.

Conclusions

In this study, the stress and fatigue of the main components of the radish collector were investigated under dynamic load conditions in order to predict the expected machine life, design, and size of the materials used in the collector. Considering the field condition, an experimental study was conducted to determine the shaft torque with and without load conditions. The Smith-Watson-Topper mean stress equation and the rain-flow-counting technique were both utilized to determine the necessary shear stress in the presence of a distribution of fatigue life cycles. The severity of the procedure was determined using Miner's rule.

Under running conditions, shear stress was found to be insignificant for the motor shafts of the stem-cutting conveyor belt, transfer conveyor belt and winch, transportation joint, and stem-cutting blade. All running conditions could produce more than 10^7 high cycle fatigue strengths. Furthermore, the highest severity levels of motor shafts for stem-cutting and transferring, transportation joint, and cutting blades were 2.20, 4.24, 2.07, and 1.07, and 1.97, 3.81, 1.73, and 1.07 with and without load conditions, respectively, aside from 5.24 for the winch motor shaft under loaded conditions.

Regarding the design parameters, for stem-cutting and transfer conveyors, increasing the diameter of the belt motor shaft resulted in lower shear stress and longer fatigue life. Although shear stress on the shaft increased, fatigue cycles were reduced when the winch motor's radial velocity was increased. The shear stress and fatigue life cycles of the transportation joint were steady across the long length side, demonstrating that this prototype is capable of working safely in the field.

The experimental findings of this study provide valuable information for the development of an automated conveyor system for radish collectors. For example, the findings may be applied to the design of appropriate radish collection conveyor components, resulting in increased design dependability while simultaneously lowering material costs.

Conflict of Interests

No potential conflict of interest to this article was reported.

Acknowledgments

This work was supported by the Korea Institute of Planning and Evaluation for Technology in Food, Agriculture, and Forestry (IPET) through the Agriculture, Food and Rural Affairs Convergence Technologies Program for Educating Creative Global Leaders, funded by the Ministry of Agriculture, Food and Rural Affairs (MAFRA) (Project No. 320001-4), Republic of Korea.

Authors Information

Khine Myat Swe, https://orcid.org/0000-0002-6565-4932
Md Nasim Reza, https://orcid.org/0000-0002-7793-400X
Milon Chowdhury, https://orcid.org/0000-0002-9887-7980

Mohammod Ali, https://orcid.org/0000-0002-1822-3005
Sumaiya Islam, https://orcid.org/0000-0003-3180-5699
Sang-Hee Lee, https://orcid.org/0000-0003-2028-9035
Sun-Ok Chung, https://orcid.org/0000-0001-7629-7224
Soon Jung Hong, https://orcid.org/0000-0003-2584-5379

References

Aldeeb T, Abduelmula M. 2018. Fatigue strength of S275 mild steel under cyclic loading. International Journal of Materials and Metallurgical Engineering 12:564-570.

Bannanttne J, Comer J, Handrock J. 1990. Fundamentals of metal fatigue analysis. Research supported by the University of Illinois. Prentice Hall, Englewood Cliffs, NJ, USA.

Chowdhury M, Islam MN, Iqbal MZ, Islam S, Lee DH, Kim DG, Jun HJ, Chung SO. 2021. Analysis of overturning and vibration during field operation of a tractor-mounted 4-row radish collector toward ensuring user safety. Machines 8:77.

Eggert L, Fricke W, Paetzold H. 2012. Fatigue strength of thin-plated block joints with typical shipbuilding imperfections. Weld World 56:119-128.

Fatemi A, Yang L. 1998. Cumulative fatigue damage and life prediction histories: A survey of the state of the art for homogenous materials. International Journal of Fatigue 20:9-34.

Fricke W, Remes H, Feltz O, Lillemäe I, Tchuindjang D, Reinert T. 2015. Fatigue strength of laser-welded thin-plate ship structures based on nominal and structural hot-spot stress approach. Ships Offshore Structure 10:39-44.

Gospodaric B, Bucar B, Fajdiga G. 2015. Active vibration control of circular saw blades. Europeon Journal of Wood and Wood Product 73:151-158.

Gujar RA, Bhaskar SV. 2013. Shaft design under fatigue loading by using modified goodman method. International Journal of Engineering Research and Applications 3:1061-1066.

Guolong Z, Jinguo Z, Hongwei W, Xubiao G, Jin Y, Likun L. 2016. Radish harvester design and finite element analysis of digging shovel. Journal of Agricultural Mechanization Research 9:94-98.

Hollomon JH. 1945. Tensile deformation. Transactions of the Metallurgical Society of AIME 162:268-290.

Islam MN, Iqbal MZ, Chowdhury M, Ali M, Shafik K, Kabir MS, Lee DH, Chung SO. 2021. Stress and fatigue analysis of picking device gears for a 2.6 kW automatic pepper transplanter. Applied Sciences 11:2241.

Jang BE, Chowdhury M, Ali M, Islam MN, Swe KM, Jung DU, Lee SH, Chung SO. 2021. Stability and vibration analysis of a tractor-mounted Chinese cabbage collector. In IOP Conference Series: Earth and Environmental Science 733:012021.

Jung HK, Kyeong UK, Yong GW. 2000. Analysis of transmission load of agricultural tractors. Journal of Terramechanics 37:113-125.

Jung YJ, Jeon HH, Jung HJ, Choi CH, Kim YJ. 2018. Finite element analysis of radish harvesting part. In 2018 ASABE Annual International Meeting. American Society of Agricultural and Biological Engineers.

Kim YJ, Chung SO, Choi CH. 2013. Effects of gear selection of an agricultural tractor on transmission and PTO load during rotary tillage. Soil & Tillage Research 134:90-96.

Köksal NS, Kayapunar A, Çevik M. 2013. Fatigue analysis of a notched cantilever beam using Ansys Workbench. In Proceedings Book of The Fourth International Conference on Mathematical and Computational Applications 8, Celal Bayar University, Manisha, Turkey.

Kolgiri S, Martande SD, Motgi N. 2013. Stress analysis for rotor shaft of electric motor. International Journal of Application or Innovation in Engineering & Management 2:136-140.

Kook HJ, Choi YS, Cho YH. 2021. Pulling performance of a self-propelled radish harvester and design of a preprocessing unit. Journal of Agriculture & Life Science 55:117-125.

Korean Society of Steel Structure. 2018. Korean steel structure design code and commentary: Load and resistance factor design. p. 773. Korean Society of Steel Structure Construction, Seoul, Korea. [in Korean].

KOSTAT (Statistics Korea). 2021. Production of autumn cabbages, autumn radishes, beans, apples and pears in 2021. Statistics Korea, Daejeon, Korea.

Lee PU, Lee NG, Choi CH, Kim YJ. 2018. Effects of working speeds of an agricultural tractor on a gear transmission. In Proceedings of the ASABE Annual International Meeting.

Li B, Zhang Z, Li W, Peng X. 2015. Model for tangential tensioning stress in the edge of circular saw blades tensioned by multi-spot pressure. BioResources 10:3798-3810.

Lillemäe I, Remes H, Romanoff J. 2013. Influence of initial distortion on the structural stress in 3 mm thick stiffened panels. Thin-Walled Structure 72:121-127.

Matejic M, Blagojevic M, Djordevic Z, Marjanovic N, Petrovic N. 2013. Comparative analysis of different type reducers for winch drum driving unit. In Proceedings of 7th International Quality Conference.

Milan S, Mária B, Miroslav B, Ján D, Juraj G. 2020. Research of the fatigue life of welded joints of high strength steel s960 ql created using laser and electron beams. Journal of Materials 13:1-19.

Miner MA. 1945. Cumulative damage in fatigue. Journal of Applied Mechanics 12:159-164.

Nguyen NT, Chu QT, Kim SE. 2011. Fatigue analysis of a pre-fabricated orthotropic steel deck for light weight vehicles. Journal of Constructional Steel Research 67:647-655.

Niu Q, Yang SX. 2018. Study on fatigue degradation behavior of a cracked rotor subjected to lateral vibration. Shock and Vibration 2018:3239523.

Petracconi CL, Ferreira SE, Palma ES. 2010. Fatigue life simulation of a rear tow hook assembly of a passenger car. Engineering Failure Analysis 17:455-463.

Piotr K. 2011. CEMA belt book. In Belt Tension Power and Drive Engineering. pp. 129-245. CEMA Publishing, Tokyo, Japan.

Radaj D, Sonsino CM, Fricke W. 2006. Fatigue assessment of welded joints by local approaches. Woodhead publishing, Hamburg, Germany.

Reza MN, Islam MN, Chowdhury M, Ali M, Islam S, Kiraga S, Lim SJ, Choi IS, Chung SO. 2021. Kinematic analysis of a gear-driven rotary planting mechanism for a six-row self-propelled onion transplanter. Machines 9:183.

Shin CS, Kim JH, Ha YS, Park T. 2019. Experimental study on the drawbar pull and structural safety of an onion harvester attached to a tractor. Journal of the Korean Society of Manufacturing Process Engineers 18:16-25.

Singh N, Singh V. 2002. Low cycle fatigue behavior of Ti alloy IMI 834 at room temperature. Materials Science and Engineering A 325:324-332.

Swe KM, Islam MN, Chowdhury M, Ali M, Wing S, Jun HJ, Lee SH, Chung SO, Kim DG. 2021a. Theoretical analysis of power requirement of a four-row tractor-mounted Chinese cabbage collector. Journal of Biosystems Engineering 46:139-150.

Swe KM, Islam MN, Jang BE, Chowdhury M, Lee SH, Jung DU, Chung SO. 2021b. Stress and fatigue analysis of the hydraulic motor shaft and conveyor joints of a tractor-mounted Chinese cabbage collector. In IOP Conference Series: Earth and Environmental Science 733:012022.

Umetsu J, Noguchi M, Matsumoto I. 1994. Measuring residual stresses in tensioned circular saws using X-rays. Mokuzai Gakkaishi 40:268-273. [in Japanese]

Wikipedia. 2021. Torsion constant. Accessed in https://en.wikipedia.org/wiki/Torsion_constant on 10 November 2021.

Yaegashi K, Osato T, Hosoda K. 2001. Performance and standard introduction for radish harvester. Tohoku Agricultural Research 54:203-204.

Yoo LN, Hwang SC. 2018. A comparative study on the policy of Korea and Japan for improving upland farming mechanization. Journal of Korean Society of Rural Planning 24:89-97.

Zhang MS, Zhang Y, Ke JJ, Li XW, Cheng LB. 2014. The influence of tangential roller pressure on the stability of circular saw blade. Applied Mechanics and Material 614:32-35.